Determination of Equation-of-State Parameters by Molecular Simulations and Calculation of the Spinodal Curve for Polystyrene/ Poly(vinyl methyl ether) Blends

Kyoungsei Choi[†] and Won Ho Jo*

Department of Fiber and Polymer Science, Seoul National University, Seoul 151-742, Korea

Shaw Ling Hsu

Department of Polymer Science and Engineering, University of Massachusetts, Amherst, Massachusetts 01003

Received March 5, 1997; Revised Manuscript Received October 28, 1997

ABSTRACT: The thermodynamic properties of polystyrene (PS) and poly(vinyl methyl ether) (PVME) are estimated using molecular dynamics and energy minimization simulations, from which the characteristic parameters of the equation-of-state are numerically evaluated. The lattice fluid theory is employed to apply the calculated characteristic parameters to the prediction of the surface tension of PS and PVME and the phase diagram of PS/PVME blends. The calculated surface tensions with no adjustable parameter agree well with the experimental data within ca. 1.0 mN/m. The calculated phase diagram of the blends is also qualitatively comparable to the experimental phase diagram.

Introduction

The lattice fluid equation-of-state theory of polymers, polymer solutions and polymer mixtures is a useful tool which can provide information on equation-of-state properties and also allows predictions of surface tensions, phase stability of polymer blends, etc.[1−4] The theory uses empty lattice sites to account for free volume, and therefore one may treat volume changes upon mixing, which are not possible in the Flory−Huggins theory. As a result, lower critical solution temperature (LCST) behaviors can, in principle, be described in polymer systems which interact chiefly through dispersion forces.[1]

Various theories have been developed to describe the effects of volume changes on polymers, polymer solutions, and mixtures, including those of Flory and coworkers,[5] Sanchez and Lacombe,[2] and Simha and Somcynski.[6] Among these, the Flory approach has been most extensively used, while the lattice fluid theory developed by Sanchez and Lacombe has been criticized since it does not afford a satisfactory description of polymer melts over a wide range of pressures.[7] Later Sanchez and Balazs[8] considered a generalized lattice fluid theory which combined the concept of specific segment interactions[9] with the earlier compressibility theory. This generalized lattice fluid theory has been applied to blends of polystyrene (PS) and poly(vinyl methyl ether) (PVME) and also to PS and tetramethylbisphenol A polycarbonate.[8,10] In this study, however, the original lattice fluid theory is adopted since it requires fewer parameters to determine the phase behavior of polymer mixtures as compared with either Flory's equation-of-state theory or the generalized lattice fluid theory.[8]

All of these equation-of-state theories involve characteristic parameters, p^*, v^*, and T^*, which have to be determined from experimental data. The least-squares fitting of density data as a function of temperature and pressure yields a set of parameters which best represent the data over the temperature and pressure ranges considered.[11] The method, however, requires tedious experiments to determine the characteristic parameters when dealing with a new polymer. Moreover, it may sometimes lead to a significant error in determining the characteristic parameters unless rigorous experimental data can be obtained. Thus, it would be helpful if the molecular simulation method[12−16] could provide the characteristic parameters without experimental efforts.

It is of our primary objective to determine the characteristic parameters of PS and PVME for the equation-of-state theory by molecular simulation and then to predict the phase diagram of PS/PVME blends as well as the surface tensions of PS and PVME.

Theory

For a polymer liquid, the lattice fluid equation-of-state can be written in a reduced form as

$$\tilde{\rho}^2 + \tilde{p} + \tilde{T}\left[\ln(1-\tilde{\rho}) + \left(1 - \frac{1}{r}\right)\tilde{\rho}\right] = 0 \qquad (1)$$

Assuming high molecular weight ($r \rightarrow \infty$) and near atmospheric pressure ($\tilde{p} \rightarrow 0$), the chemical potential μ is given by

$$\mu = -\tilde{\rho} + \tilde{T}\frac{(1-\tilde{\rho})\ln(1-\tilde{\rho})}{\tilde{\rho}} \qquad (2)$$

where ρ is density, p is pressure, v is volume, T is temperature, and r is molecular size parameter. The chemical potential, density, pressure, and temperature

* To whom correspondence should be addressed.
[†] Present address: R&D Center, Samsung Cheil Industries Inc., 332-2, Gochun-dong, Euiwang-shi, Kyoungki-do, Korea.

S0024-9297(97)00300-8 CCC: $15.00
Published on Web 01/31/1998

are reduced by their respective equation-of-state parameters as follows:

$$\tilde{\mu} = \frac{\mu}{rNkT^*},$$

$$\tilde{\rho} = \frac{\rho}{\rho^*} = \frac{1}{\tilde{v}} = \frac{v^*}{v},$$

$$\tilde{p} = \frac{p}{p^*},$$

$$\tilde{T} = \frac{T}{T^*} \tag{3}$$

For polymer liquids, the gradient approximation in conjunction with the lattice fluid model has been used to calculate surface tensions.[17,18] The density profile can be determined by integrating the Euler−Lagrange equation

$$\tilde{x} - \tilde{x}_0 = \int_{\tilde{\rho}_0}^{\tilde{\rho}} (\tilde{\kappa}/\Delta a)^{1/2}\, \mathrm{d}\tilde{\rho} \tag{4}$$

where the subscript 0 denotes an arbitrary reference point, x is a position along the line vertical to the surface, and $\tilde{\kappa}$ is a dimensionless constant. The $\tilde{\kappa}$ has a priori theoretical value of 0.5. The Cahn−Hilliard relation for surface tension σ, in terms of reduced variables, can be expressed as

$$\tilde{\sigma} = 2\int_{\tilde{\rho}_g}^{\tilde{\rho}_l} (\tilde{\kappa}/\Delta\tilde{a})^{1/2}\, \mathrm{d}\tilde{\rho} \tag{5}$$

where

$$\Delta\tilde{a} = \tilde{\rho}[\tilde{\mu}(\tilde{\rho},\tilde{T}) - \tilde{\mu}(\tilde{\rho}_l,\tilde{T})] \tag{6}$$

$$\tilde{\sigma} = \frac{\sigma}{(kT^*)^{1/3}(p^*)^{2/3}}, \qquad \tilde{x} = \frac{x}{(v^*)^{1/3}} \tag{7}$$

The subscripts, g and l, in eq 5 denote the gas state and the liquid state, respectively. By substituting eq 2 into eq 6, and then integrating eq 4 and eq 5, the density profile and the surface tension can be obtained, respectively. Such a procedure has previously been shown to yield estimates of surface tension for polyethylene melts in good agreement with experiment.[19]

For simplicity, assuming that the close-packed volume of a PS-mer (v^*_{PS}) is equal to that of a PVME-mer (v^*_{PVME}), the binary polymer blend is miscible[4] when

$$f_{\phi\phi} = \left(\frac{\partial^2 f}{\partial \phi_{PS}^{\ 2}}\right) = f_{\phi\phi,1} + f_{\phi\phi,2} < 0$$

$$f_{\phi\phi,1} = 2\,\tilde{\rho}\phi_{PS}\,\phi_{PVME}\,\chi$$

$$f_{\phi\phi,2} = \tilde{\rho}\phi_{PS}\,\phi_{PVME}\,\tilde{T}\,\Psi^2\,p^*\beta \tag{8}$$

where f is the free energy per mer, ϕ_i is the volume fraction of component i, β is the isothermal compressibility of the mixture, and the interaction energy parameter χ is expressed as eq 9:

$$\chi = (\epsilon^*_{PS} + \epsilon^*_{PVME} - 2\epsilon^*_{PS:PVME})/kT \tag{9}$$

$$\epsilon^*_{PS} = kT^*_{PS},$$

$$\epsilon^*_{PVME} = kT^*_{PVME},$$

$$\epsilon^*_{PS:PVME} = \sqrt{\epsilon^*_{PS}\,\epsilon^*_{PVME}} \tag{10}$$

More detail description for eq 8, including the definition of Ψ, can be found elsewhere.[1,4]

Model and Simulation

The commercial software Cerius[2] from Molecular Simulations, Inc., is used and the force field UNIVERSAL[20] is adopted in this work. The intramolecular interactions are described by terms such as bond, bending, torsion, and inversion and the intermolecular interactions by terms such as van der Waals and electrostatic. The nonbonded interactions are calculated using the Ewald method.[12] The monomeric unit of PS is modeled to have a total charge of zero, and the distribution of the partial charge in the monomer is determined by the charge equilibration method.[21]

An atactic PS chain with 20 repeating units is generated to have 50% of the meso diad fraction, and then packed into a cubic simulation box with the three-dimensional periodic boundary, where the torsional angles are randomly created. The initial size of the cubic box is chosen to have the density of 1.0 g/cm^3. The energy of the PS structure is roughly minimized, and then the structure is relaxed by performing *NVT*-molecular dynamics at 1 000 K for 100 000 steps (1 step corresponds to 1 fs) to overcome the local minimum energy barrier. The structure is equilibrated by *NpT*-molecular dynamics at 400 K for 100 000 steps, and then *NpT*-molecular dynamics at 300 K for 100 000 steps where the coordinates are stored at every 200 steps for the confirmation of the equilibration and analysis. The equilibration is monitored by the total energy and the volume of the simulation box because these two quantities are the most important in this study. The six equilibrated structures extracted from the molecular-dynamics trajectory at 300 K are energy-minimized for both the coordinates of the atoms and the cell parameters.[22] After the minimization is converged, a short time *NVT*-molecular dynamics starts at high temperature. This minimization procedure followed by a short time *NVT*-molecular dynamics is repeated three times. After the final minimization, the close-packed state at 0 K is obtained. It is reported that the energy-minimization results are almost independent of the initial temperature of the model polymer.[19,22] Thus, the initial models for energy minimization are prepared only at 300 K in this simulation. The same procedures are also applied to the PVME.

The distribution of charges could be affected by a large change in chain conformation during molecular dynamics. Therefore, it may be worthwhile to add a charge equilibration step before the last energy minimization so as to obtain more improved results. However, the second step for charge equilibration is not performed in this study, because the conformation is not changed significantly during the structure equilibration in usual

Table 1. Hildebrand Solubility Parameters in $MPa^{1/2}$

		400 K	300 K	0 K
PS	simul	17.74 ± 0.28	18.63 ± 0.29	20.36 ± 0.14
	literature		18.5[a]	
			18.5[b]	
PVME	simul	17.71 ± 0.67	19.19 ± 0.57	21.11 ± 0.44
	literature		18.4[c]	
			19.2[d]	

[a] Preferred value from ref 24. [b,d] Calculated value using group contribution technique by Ahmad and Yaseen from refs 25 and 27, respectively. [c] Mean literature value from ref 26.

molecular simulations, and furthermore the charge equilibration for polymers is very time-consuming.

The thermodynamic properties at 300 and 400 K are calculated by time averaging. The reproducibility is confirmed by performing other molecular dynamics and energy minimization starting from other initial configurations and comparing the simulated properties with each other. The distribution of torsional angles in the chain backbone is examined to confirm the conformational equilibration of the structures, which are initially produced to have a random distribution of torsional angles.

In summary, the volume−temperature and energy−temperature data are calculated from the results of the NpT-molecular dynamics, and the close-packed state at 0 K is directly obtained from the energy minimization. The characteristic parameters are then evaluated by a simple analysis of the simulation results.

The Hildebrand solubility parameters and densities of PS and PVME are calculated and compared with the experimental data to confirm the validity of the force field. The Hildebrand solubility parameter is the square root of the cohesive energy density which is defined as the energy difference when a polymer of unit volume is evaporated in a vacuum. The solubility parameters are obtained for the seven structures extracted from the trajectory and averaged by following the standard method.[23]

Results and Discussion

Table 1 shows the simulated Hildebrand solubility parameters of PS and PVME. The literature values of solubility parameter for PVME lie in a broad range of 16−20 $MPa^{1/2}$, and the mean value of PVME is estimated to be 18.4 $MPa^{1/2}$. The simulated solubility parameters of both PS and PVME fall into the experimental range and agree well especially with the ones calculated using the group contribution technique. The densities obtained by molecular simulations also agree well with the experimental values as shown in Table 2, although the densities obtained by molecular simulations are slightly lower than the experimental values. The derivative of density with respect to temperature shows the same qualitative trend as that of the experimental one although the number of samples for the calculation is not sufficient. Molecular dynamics and energy minimization for polymers are not ergodic, and thus the result may strongly depend on the initial structure. Therefore, it is necessary to examine the reproducibility of the simulated quantities. For this purpose, we calculated the solubility parameter and density from other initial structure and compared the values with experimental ones. The solubility parameters of PS and PVME at 0 K were 20.62 $MPa^{1/2}$ and 21.90 $MPa^{1/2}$, respectively, and the densities of PS and PVME at 0 K were 1.083 and 1.068 g/cm^3, respectively, when the systems are simulated from other initial structures. These results also fall into the acceptable range, indicating that the simulated results are reproducible.

Since v_{sp}^* is defined as the specific volume at close-packed state and p^* is equal to ϵ^*/v^*, that is, the cohesive energy density at close-packed state,[1] the specific volume at 0 K corresponds to v_{sp}^*, and the cohesive energy density at 0 K to p^*. The T^* is obtained by inserting p^*, v_{sp}^*, and simulated (T, v_{sp}) data at room temperature into the lattice fluid theory. The absolute value of simulated equation-of-state parameters may not be the same as that of the experimental one (Table 3) because the procedures obtaining the parameters are different from each other. They are, however, comparable to experimentally determined values. The relative magnitude of the characteristic parameters for two polymers has been well produced in the simulation, which is very important for determining the shape of the phase diagram and the qualitative trend of surface tension.

The initial structures of PS and PVME are produced to have a random distribution of torsional angles, as shown in Figure 1. However, it should be mentioned that the initial torsional angles are chosen to avoid serious physical overlaps of the atoms, and thus their distributions may not be random in a strict sense. The distribution after equilibration is prepared from a 60 ps long trajectory, which shows some remarkable peaks. The 0 degree in Figure 1 corresponds to cis-state, which is unfavorable because of the repulsive forces between chain segments.

Figure 2 shows the temperature dependence of the surface tension. The differences between calculated values and the experimental ones do not exceed ca. 1 mN/m (1 mN/m is equal to 1 dyn/cm). Here we do not use an adjustable parameter, assuming that the $\tilde{\kappa}$ does not vary with the temperature and is fixed at 0.5, the theoretical value for both PS and PVME. The temperature derivatives of the surface tensions also agree well with the experimental values, as shown in Table 4. As can be seen in Table 3, the PS and PVME have similar equation-of-state parameters such that both polymers are expected to have similar density profiles (Figure 3). However, a closer examination of Figure 3 reveals that the density profile of PVME at surface becomes slightly broader than that of PS and that the equilibrium liquid density of PVME is slightly lower than that of PS, since the thermal expansivity of PVME is higher than that of PS (see Table 2). This confirms the experimental observations that PS and PVME have similar densities

Table 2. Densities (g/cm^3) and $d\rho/dT$ (g/cm^3 K)

		400 K	300 K	0 K	$d\rho/dT$
PS[a]	simul	1.002 ± 0.019	1.024 ± 0.016	1.079 ± 0.006	-1.90×10^{-4}
	exp[b]		1.04−1.065		-2.65×10^{-4}
PVME[c]	simul	0.965 ± 0.028	1.012 ± 0.019	1.075 ± 0.009	-4.7×10^{-4} [d]
	exp[e]	0.982	1.053		-7.1×10^{-4}

[a] T_g = 80−100 °C. [b] From ref 28. [c] T_g = −34 °C, T_m = 144 °C. [d] Calculated value only for above T_g. [e] From ref 29.

Table 3. Equation-of-State Parameters

		p^*(MPa)	v^*_{sp} (cm^3/g)	T^*(K)
PS	simul	415 ± 6	0.927 ± 0.006	676
	exp[a]	357	0.905	735
PVME	simul	446 ± 18	0.930 ± 0.007	639
	exp[b]	363	0.909	657

[a] From ref 5. [b] From ref 6.

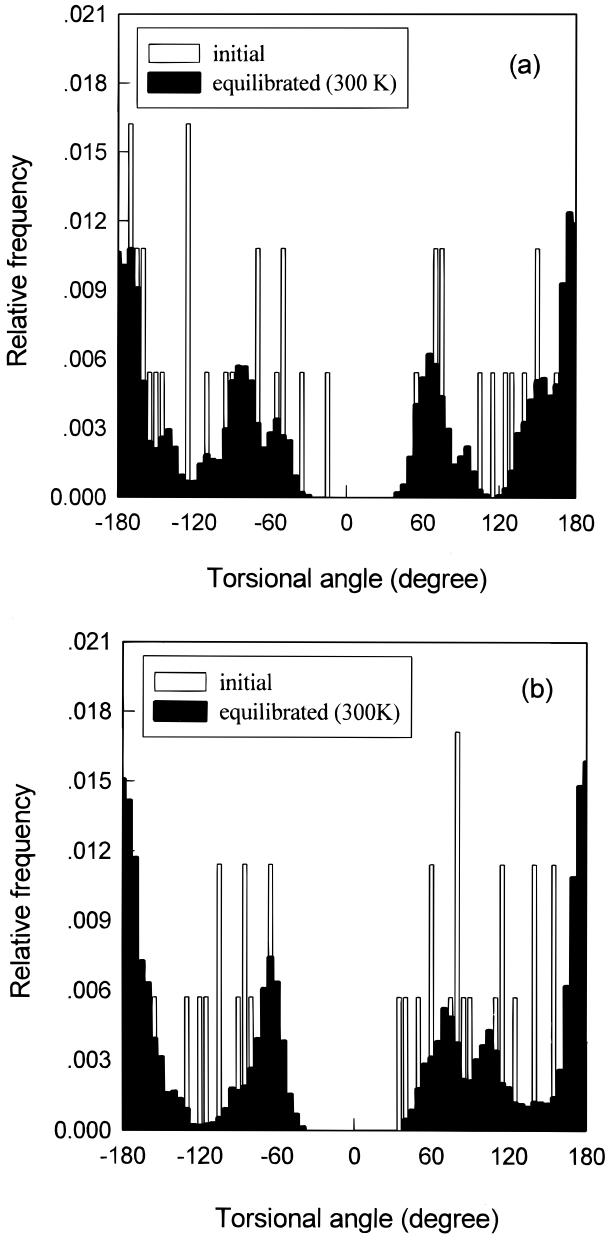

Figure 1. Distribution of torsional angles in the chain backbone at the initial and the equilibrium state for (a) PS and (b) PVME. Two kinds of torsional angles with asymmetric distribution are summed together for both PS and PVME.

but that PVME has a lower density than PS at higher temperature.

From the above results on the solubility parameter, density, thermal expansivity, surface tension, and equation-of-state parameters, the simulation method adopted here has been validated for PS and PVME homopolymers, although the size of the system box in this study seems to be small. Two of the most important properties in this study are density and cohesive energy, which may not be strongly affected by the system size and thus well equilibrated with acceptable fluctuations when the NpT-molecular dynamics is performed.

It has been known that the LCST behaviors originated from the specific interactions between components

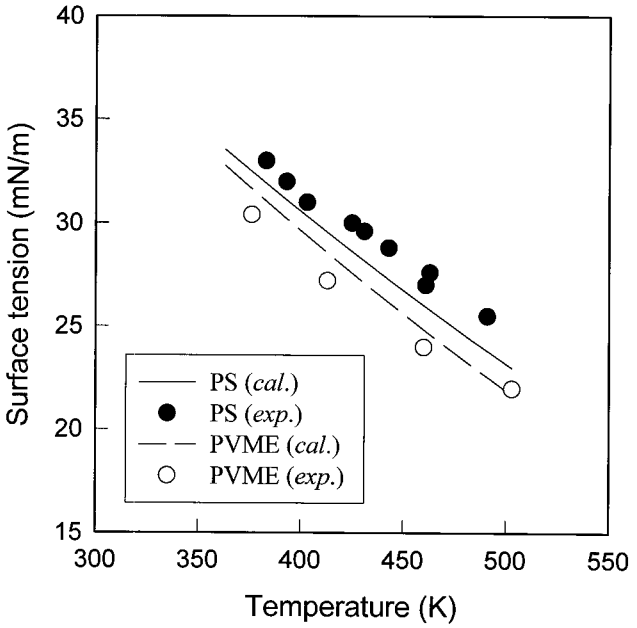

Figure 2. Temperature dependence of surface tension of PS and PVME. The circles represent the experimental data,[30] and the lines are the calculated values using the simulated equation-of-state parameters. The dimensionless constant $\tilde{\kappa}$ in eq 4 is fixed at a theoretical value of 0.5 such that there is no adjustable parameter.

Table 4. dσ/dT in MN/MK

	dσ/dT	
	calcd	expt[a]
PS	−0.075 (0.999)[b]	−0.068 (0.988)
PVME	−0.079 (0.999)	−0.066 (0.984)

[a] From ref 30. [b] Square of correlation coefficient.

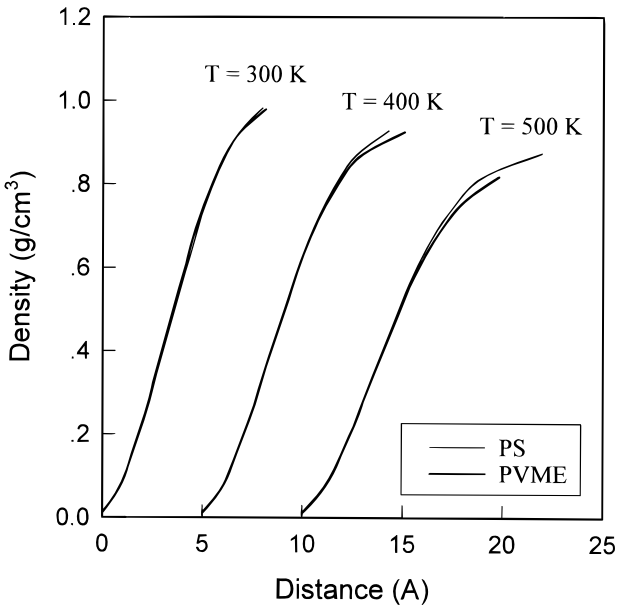

Figure 3. Density profile of PS and PVME at the surface. The origin is assigned arbitrarily and the profiles at 400 and 500 K are shifted to the left by 5 and 10 Å, respectively, for clarity. The left side of the profile corresponds to the vapor and the right side to the liquid.

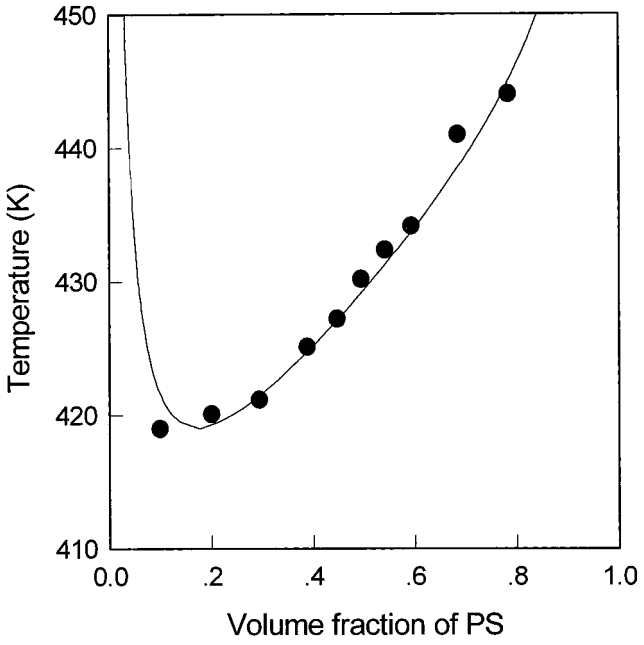

Figure 4. Phase diagram of PS/PVME blend. The line represents the calculated results using the simulated equation-of-state parameters with $\zeta = 1.000\ 66$. Filled circles represent experimental spinodal data.[33]

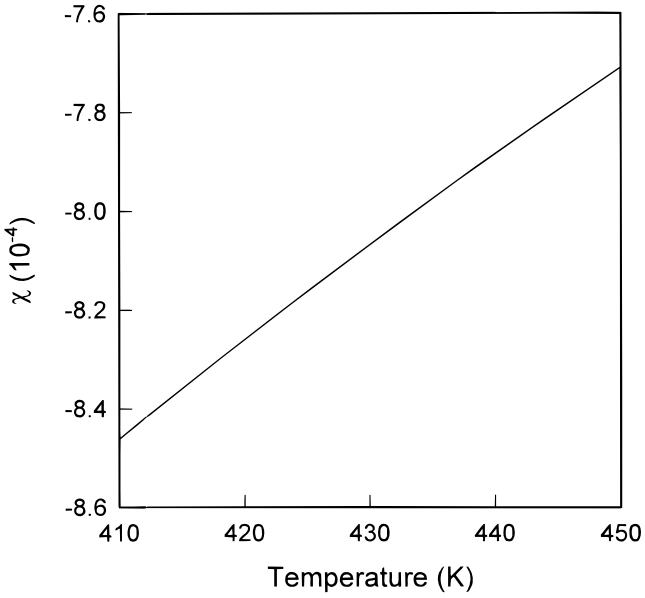

Figure 5. Temperature dependence of interaction energy parameter for PS/PVME blend when the value of $\zeta = 1.000\ 66$ for the best fit is used.

and/or the finite compressibility of mixture and that the phase separation is entropically driven in either case. Determination of the interaction parameter between PS and PVME is essential to predict the phase diagram using the equation-of-state theory. The interaction between PS and PVME can be represented by a dimensionless parameter ζ in eq 10, but this mixing rule can be applied only to the situation where the dispersion force is dominant, that is, there is no remarkable specific interaction. Although the evidence of the specific interactions between PS and PVME has been reported,[5,29,31] it has been presumed that there is only weak specific interaction between PS and PVME, and therefore Flory's equation-of-state theory, in which specific interactions are not taken into account, could be applied to the system.[29] In this work, the extent of the specific interaction is also assumed to be weak enough for the original lattice fluid theory to be applied. The parameter ζ might be simulated by the so-called docking method[32] where each ϵ_i (i = PS, PVME, or PS: PVME) is calculated and then one can determine the value of ζ directly from eq 10. But, ζ is too sensitive to extract an exact value from the method without any flexibility. Thus, the critical temperature in the phase diagram is fitted to the experimental one by varying ζ (Figure 4). The best fit is obtained when $\zeta = 1.000\ 66$. The parameter ζ, slightly larger than the unity, leads to a slightly negative χ, as shown in Figure 5. The shape of calculated spinodal agrees well with the experimental one, indicating that the determination of the equation-of-state parameters from molecular simulations and some assumptions adopted here are reasonable.

The theoretical treatment accounting for nonrandom mixing which may be induced by the specific interactions was first carried out by Guggenheim.[34] Sanchez and Balazs[8] have generalized the lattice fluid model by introducing the idea of specific interaction in an incompressible binary blend into the original lattice fluid theory. However, the generalized lattice fluid theory has more parameters to be fitted than the original theory. It is very significant that the spinodal curve could be successfully predicted by using only one adjustable parameter when simulated values of equation-of-state parameters are used, considering that the original lattice fluid theory predicts a very narrow spinodal curve when experimental values of equation-of-state parameters are used with one adjustable parameter.[8] Better prediction by using simulated parameters may arise from the self-consistency between parameters. In experiments, each parameter is determined independently. More specifically, v^*_{sp} and p^* are determined by measuring the thermal coefficient and the thermal pressure coefficient, respectively, so that the consistency between parameters cannot be directly examined. But, the simulated parameters are self-consistent, because v^*_{sp} and p^* are directly determined respectively from the specific volume and the cohesive energy of the same simulation box at 0 K.

When some conditions such as infinite molecular weight, near atmospheric pressure, and $v^*_{PS} = v^*_{PVME}$ are assumed, the simplified equation-of-state in eq 8 leads to an easy interpretation on the phase diagram. Figures 6 and 7 show the components of the second derivative of the free energy per mer in eq 8 as a function of temperature and composition, respectively. The first term in eq 8, the enthalpic contribution slightly decreases in magnitude with increasing temperature and is symmetric with respect to the volume fraction of the PS. The second term, the compressibility contribution slightly increases with the temperature and is asymmetric with respect to the volume fraction of PS. This asymmetry leads to the asymmetric shape of the phase diagram, where the critical point for a LCST is rich in PVME with the lower T^*. The total sum results in the immiscibility at higher temperatures and PVME-rich region. In this system, both the specific interaction shown by the negative interaction parameter and the compressibility play important roles in developing the LCST behavior.

In this study, the p^* and v^* are uniquely determined by the molecular simulation method, but the T is a function of temperature because the T^* is determined

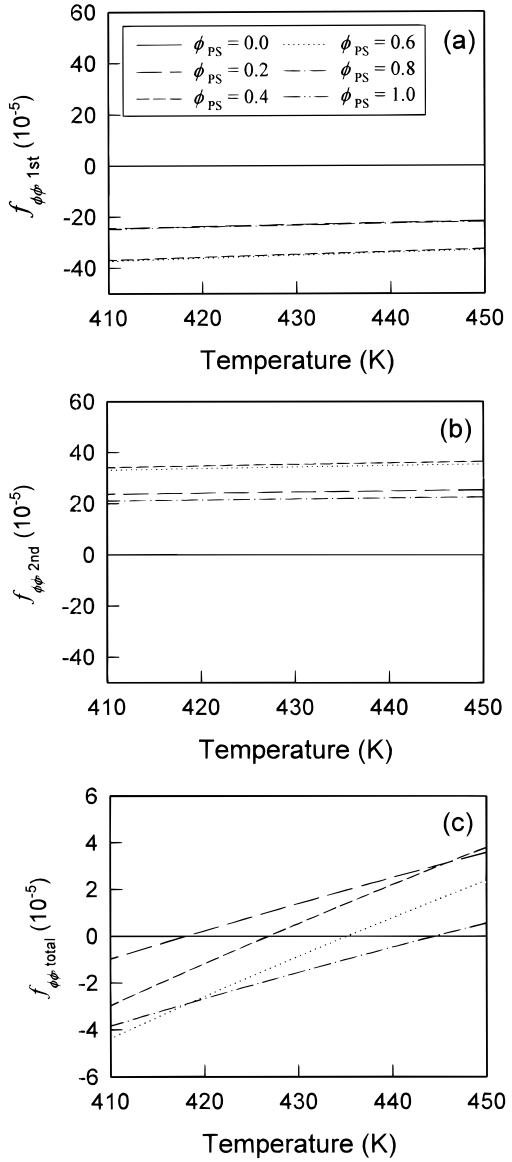

Figure 6. The second derivative of the free energy as a function of temperature: (a) the first term in eq 8; (b) the second term; (c) the total.

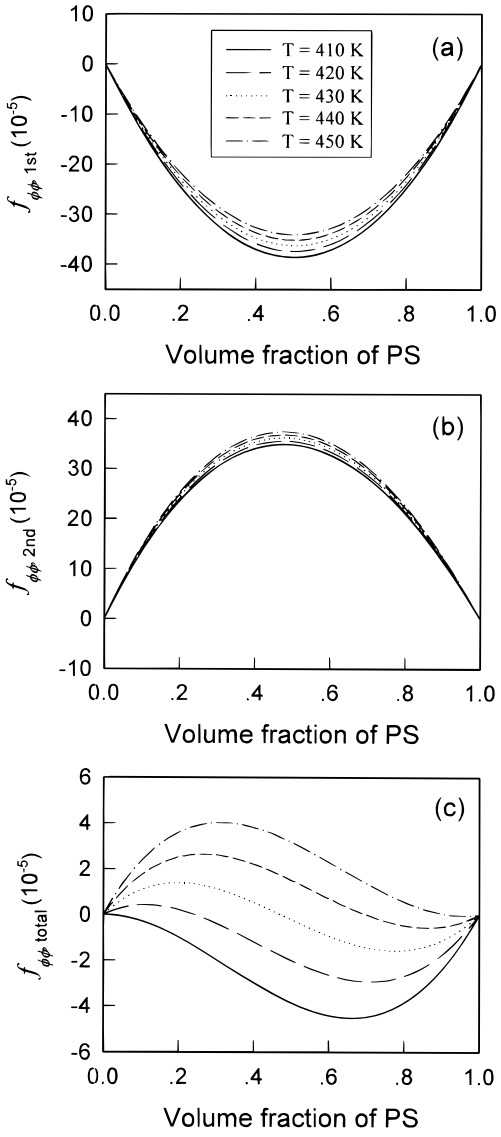

Figure 7. Second derivative of the free energy as a function of composition: (a) the first term in eq 8; (b) the second term; (c) the total.

by a set of T and v_{sp}. This is a similar situation to the experimental one which has a different set of equation-of-state parameters over a certain range in temperature and pressure. We have assumed T^* to be independent of temperature and used the value at 300 K to simulate the phase diagram. This assumption may result into an error, despite the fact that we have successfully predicted the phase diagram of PS/PVME blends. To avoid relying on the adjustable parameter, the exact description of ζ must be made. For the purpose, the quantum chemical approach to the pairwise interaction may provide a solution to the problem, which remains to be solved in the future.

Conclusions

The thermodynamic properties are calculated by molecular dynamics and energy minimization, from which the characteristic parameters of the equation-of-state theory, p^*, v_{sp}^*, and T^* are determined based on the physical meaning of the parameters. In this study, the lattice fluid theory with simulated characteristic parameters is used for the prediction of the surface tension and the phase diagram. The calculated surface tensions of PS and PVME with no adjustable parameter agree well with the experimental data within ca. 1.0 mN/m, indicating that the simulated equation-of-state parameters for the pure polymers are reasonable. The calculated phase diagram of PS/PVME blends is also comparable to the experimental one with the use of an adjustable parameter ζ. The parameter ζ leads to a reasonable interaction energy parameter for this system with weak specific interactions. However, there still remain some improvements. The temperature dependence of T^* needs to be incorporated into the equation-of-state, and the simulation method to yield an exact interaction energy parameter should be explored for a more definite prediction of the phase behavior of polymer blends.

Acknowledgment. W. H. Jo thanks the Ministry of Education, the Republic of Korea, for their financial support.

References and Notes

(1) Sanchez, I. C. In *Polymer Blends*; Paul, D. R., Ed.; Academic Press: New York, 1978.

(2) Sanchez, I. C.; Lacombe, R. H. *J. Phys. Chem.* **1976**, *80*, 2352.
(3) Sanchez, I. C.; Lacombe, R. H. *Macromolecules* **1978**, *11*, 1145.
(4) Lacombe, R. H.; Sanchez, I. C. *J. Phys. Chem.* **1976**, *80*, 2568
(5) Walsh, D. J.; Dee, G. T.; Halary, J. L.; Ubiche, J. M.; Millequant, M.; Lesec, J.; Monnerie, L. *Macromolecules* **1989**, *22*, 3395 and references therein.
(6) Simha, R.; Somcynski, T. *Macromolecules* **1969**, *2*, 342.
(7) Zoller, P. *J. Polym. Sci.: Polym. Phys. Ed.* **1980**, 18, 897; *J. Polym. Sci.: Polym. Phys. Ed.* **1980**, *18*, 157.
(8) Sanchez, I. C.; Balazs, A. C. *Macromolecules* **1989**, *22*, 2325.
(9) ten Brinke, G.; Karasz, F. E. *Macromolecules* **1984**, *17*, 815.
(10) Kim, E.; Kramer, E. J.; Osby, J. O.; Walsh, D. J. *J. Polym. Sci., Part B: Polym. Phys.* **1995**, *33*, 467.
(11) Sanchez, I. C.; Lacombe, R. H. *J. Polym. Sci. Polym. Lett. Ed.* **1977**, *15*, 71.
(12) Allen, M. P.; Tildesley, D. J. *Computer Simulation of Liquids*; Clarendon Press: Oxford, 1987.
(13) Monnerie, L., Suter, U. W., Eds. *Advances in Polymer Science 116*; Springer-Verlag: Berlin, 1994.
(14) Burkert, U.; Allinger, N. L. *Molecular Mechanics*; American Chemical Society: Washington, DC, 1982.
(15) Roe, R. J., Ed. *Computer Simulation of Polymers*; Prentice Hall: Englewood Cliffs, NJ, 1991.
(16) Binder, K.; Heermann, D. W. *Monte Carlo Simulation in Statistical Physics*; Springer-Verlag: Berlin, 1988.
(17) Poser, C. I.; Sanchez, I. C. *J. Colloid Interface Sci.* **1979**, *69*, 539.
(18) Sanchez, I. C. In *Physics of Polymer Surfaces and Interfaces*; Sanchez, I. C., Ed.: Butterworth-Heinemann: Oxford and Woburn, 1992.
(19) Jo, W. H.; Choi, K. *Macromolecules* **1997**, *30*, 1800.
(20) Rappé, A. K.; Casewit, C. J.; Colwell, K. S.; Goddard, W. A., III; Skiff, W. M. *J. Am. Chem. Soc.* **1992**, *114*, 10024.
(21) Rappé, A. K.; Goddard, W. A., III *J. Phys. Chem.* **1991**, *95*, 3358.
(22) Boyd, R. H.; Pant, P. V. K. *Macromolecules* **1991**, *24*, 4078.
(23) Theodorou, D. N.; Suter, U. W. *Macromolecules* **1985**, *18*, 1467.
(24) Barton, Allan F. M. *CRC Handbook of Polymer-Liquid Interaction Parameters and Solubility Parameters*; CRC Press: Boca Raton, FL, 1990.
(25) Ahmad, H.; Yaseen, M. *Polym. Eng. Sci.* **1979**, *19*, 858.
(26) Allen, S. M.; Stannett, V.; Hopfenberg, H. B. *Polymer* **1981**, *22*, 912.
(27) Ahmad, H.; Yaseen, M. *J. Oil Colour Chem. Assoc.* **1977**, *60*, 99.
(28) Brandrup, J., Immergut, E. H., Eds. *Polymer Handbook*, 3rd ed.; John Wiley & Sons: New York, 1989.
(29) Shiomi, T.; Hamada, F.; Nasako, T.; Yoneda, K.; Imai, K.; Nakajima, A. *Macromolecules* **1990**, *23*, 2296
(30) Dee, G. T.; Sauer, B. B. *Macromolecules* **1993**, *26*, 2771.
(31) Garcia, D. *J. Polym. Sci., Polym. Phys. Ed.* **1984**, *22*, 1733.
(32) Choi, K.; Jo, W. H. *Macromolecules* **1997**, *30*, 1509 and references therein.
(33) Han, C. C.; Baurer, B. J.; Clark, J. C.; Muroga, Y.; Matsushita, Y.; Okada, M.; Tran-Cong, Q.; Chang, T.; Sanchez, I. C. *Polymer* **1988**, *29*, 2002.
(34) Guggenheim, E. A. *Proc. R. Soc. London* **1935**, *A148*, 304.

MA970300+